Numerical discovery and experimental validation of vortex ring generation by microramp vortex generator

Qin Li, Ping Lu, Chaoqun Liu, Adam Pierce, and Frank Lu

1 Introduction

Micro vortex generators are a new kind of passive flow control instruments for shock-boundary layer interaction problems. In contrary to the conventional vortex generator, they have heights approximately 20-40% (more or less) of the boundary layer. Among them, Mircoramp vortex generators (MVG) are given special interest by engineers because of their structural robustness. The mechanism of the flow control was thought that a pair of streamwise vortex is generated by MVG and remains in the boundary layer for relatively long distance; the down-wash effect by the streamwise vortices will bring about momentum exchange, which makes the boundary layer less liable to separation. During such process, a specific phenomenon called as momentum deficit will happen [1], i.e., a cylindrical region consisted of low speed flows will be formed after the MVG. It was pointed out by Li and Liu [2] that the origin of deficit comes from the shedding of boundary layer over MVG.

Numerical simulations have been made on MVG for comparative study and further design purposes. Ghosh, Choi and Edwards [3] made detailed computations under the experimental conditions given by Babinsky by using RANS, hybrid RANS/LES and immersed boundary (IB) techniques. Lee et al [4, 5] also made computations on the micro VGs problems by using Monotone Integrated Large Eddy Simulations (MILES). Basic flow structures like momentum deficit and streamwise vortices were reproduced in the computation. Further studies were also conducted on the improvement of the control effect.

It is definitely needed to find physics of MVG for design engineers. RANS, DES, RANS/DES, RANS/LES, etc are good engineering tools, but may not be able to reveal the mechanism and get deep understanding of MVG. We need high order DNS/LES. A powerful tool is the integration of high order LES and experiment. An implicit large eddy simulation was conducted on the MVG controlled flow at

University of Texas at Arlington, 701 S. Nedderman Drive, Arlington, TX 76019, USA

Mach number 2.5. Flows of MVGs are studied with back edge declining angle (see Figure 1 (left)).The geometries for the cases are shown in Figure 1 (right). The details about the geometric objects, grid generation, computational domain, etc, are introduced in our previous paper [3, 6] and will not be repeated here. Through the computation, a new phenomenon called as vortex rings was first discovered, i.e., a train of vortex rings will be generated continuously within the boundary of the momentum deficit. The mechanism for the vortex rings was analyzed and found that, the existence of the high shear layer and inflection surface generated by the momentum deficit will cause the corresponding Kelvin-Helmholtz instability, which develops into a series of vortex rings. An experiment was designed to validate the discovery. The snapshot of the laser sheet at the center plane demonstrated the vortex structures after MVG and confirmed the discovery by our LES.

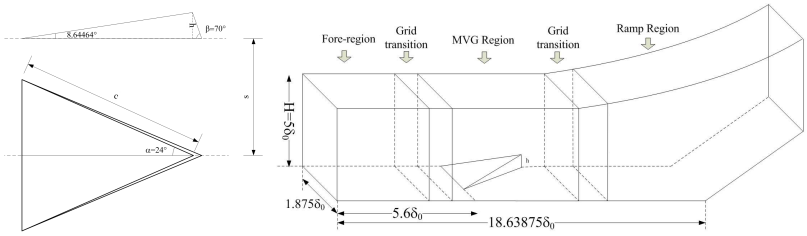

Fig. 1 Left: the sketch of MVG at $b = 70^\circ$, right: the schematic of the half grid system.

2 Numerical Method

In this paper, we investigate vortex ring generation by microramp vortex generator at $M = 2.5$ and $Re_\theta = 5760$. A kind of large eddy simulation method is used by solving the unfiltered form of the Navier-Stokes equations with the 5^{th} order Bandwidth-optimized WENO scheme [7], which is generally referred to the so-called implicitly implemented LES [8]. Without explicitly using the subgrid scale (SGS) model as the explicit LES, the implicitly implemented LES uses the intrinsic dissipation of the numerical method to dissipate the turbulent energy accumulated at the unresolved scales with high wave numbers.

The adiabatic, zero-gradient of pressure and non-slipping conditions is adopted at the wall. To enforce the free stream condition, fixed value boundary condition with the free parameters is used on the upper boundary. The boundary conditions at the front and back boundary surface in the spanwise direction are treated as the mirror-symmetry condition, which is under the consideration that the problem is about the flow around MVG arrays and only one MVG is simulated. The outflow boundary conditions are specified as a kind of characteristic-based condition, which can handle the outgoing flow without reflection [3].

The inflow conditions are generated using the following steps:

1. A turbulent mean profile is obtained from previous DNS simulation result [9] for the streamwise velocity (w-velocity) and the distribution is scaled using the local displacement thickness and free stream velocity. The basic transfer is based on the assumption that the same distribution exists between the relations of $U/U_e \sim y/\delta^*$. And the averaged streamwise velocity of MVG case can be got by interpolation (3^{rd} spline interpolation).
2. The pressure is uniform at inlet and is the same as the free stream value. The temperature profile is obtained using Walz's equation for the adiabatic wall: first the adiabatic wall temperature is determined using: $T_w = T_e\left[1 + r\left(\gamma - 1\right)/2M_e^2\right]$, where the subscript e means the edge of the boundary layer and r is the recovery factor with value 0.9; next the temperature profile is obtained by Walz's equation: $T/T_e = T_w/T_e - r\left(\gamma - 1\right)/2M_e^2\left(U/U_e\right)^2$.
3. The fluctuation components of the velocity are separated from the velocity at every instantaneous data file (total 20000 files). And such fluctuations are rescaled in the same way. Because $\overline{T}/T_e = T_w/T_e - r\left(\gamma - 1\right)/2M_e^2\left(\overline{U}/U_e\right)^2$, considering the non-dimensional form and ignore the T_e and U_e, we get $\mathrm{d}\overline{T} = -r\left(\gamma - 1\right)M_e^2 U\mathrm{d}\overline{U}$, or $\Delta T = -r\left(\gamma - 1\right)M_e^2 U\Delta U$. Density fluctuation is determined by $\Delta\rho/\overline{\rho} = -\Delta T/\overline{T}$.
4. Finally, the transformed parameters are $u = U + \Delta u$, $v = V + \Delta v$, $w = \Delta w$, $\rho = \overline{\rho} + \Delta\rho$, $p = \rho T/\left(\gamma M^2\right)$ and $T = \overline{T} + \Delta T$.

3 Inflection Surface, K-H instability and Vortex Ring Generation by MVG

3.1 Inflection surface in 3-D flow behind MVG

In order to explore the mechanism of the vortex ring generation, the distributions of averaged streamwise-velocity are given in Figure 2(left) along the normal grid lines at the center plane. The streamwise positions of the lines are $L_{from\,apex}/h \approx 3.3, 6.7, 10$ and 11, where $L_{from\,apex}$ is the streamwise distance measured from the apex of MVG. The dip of the lines corresponds to the momentum deficit. From the results, it can be seen clearly that there are at least two high shear layers in the central plane, one is located at the upper edge of the dip and the other is located at the lower edge. Within the shear layer, there is at least one inflection point. In order to demonstrate the existence of the inflection points, the second order derivative $\partial^2 w/\partial y^2$ (w is the stremwise velocity and y is the normal direction) is calculated along the lines, and the result of the line at $L_{from\,apex}/h \approx 6.7$ is plotted in Figure 2 (center and right) as an example. The existence and correspondence of the inflection points at the upper and lower shear layers is illustrated by two dashed lines intersecting the distribution of the streamwise velocity and its second order derivative.

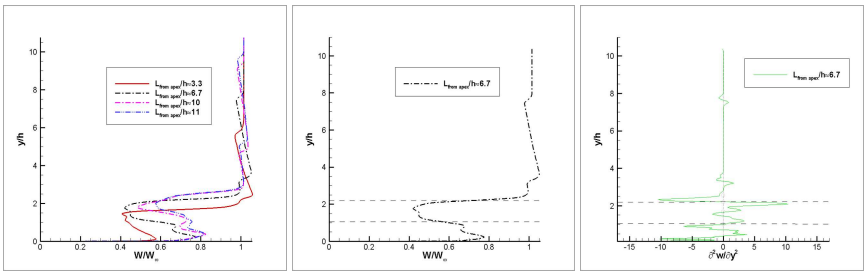

Fig. 2 Left:Averaged streamwise velocity at different sections. Inflection points (surface for 3-D). Center: averaged stremwise velocity at $L_{from\ apex}/h \approx 6.7$, right: $\partial^2 u/\partial y^2 = 0$.

3.2 Vortex ring generation

Based on the above analyses, it can be concluded that the existence of the inflection points (surface in 3-D) in the shear layer causes the flow instability and generates vortex rollers by K-H instability in a cylindrical coordinate system. Therefore, the mechanism of the vortex ring generation should be K-H instability. The lost of the stability of the shear layer will result in the roll-up of the vortex, which appears in ring-like structure in a 3-D view (Figure 3). In Figure 3 (b), λ_2 is certain eigenvalue of the stress tensor, and its iso-surface is usually used to describe the vortex surface. The intensity of the upper shear layer appears to be stronger than that of the lower shear layer (Figure 3). In Figure 4, another qualitative checking about the shear layer

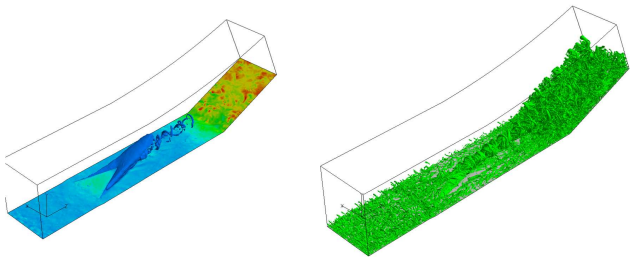

Fig. 3 Vortex ring generation by MVG due to K-H instability. Left: iso-surface of pressure, right: iso-surface of λ_2.

and K-H instability is made by using the instantaneous flow field. In the figure, the background at the central plane and the spanwise plane is colored by the value of the streamwise velocity, so that the green regions in two planes represent the momentum deficit. In the central plane, the pressure contours are superimposed on the background cloud-map. The figure shows that, the blue circle structures, which indicate the core of the ring like vortices cut by the plane, are located on the boundary of the deficit circle. Such positions are exactly the same place where the high shear

layer exists. In Figure 5, we give the instantaneous numerical schlieren picture at the

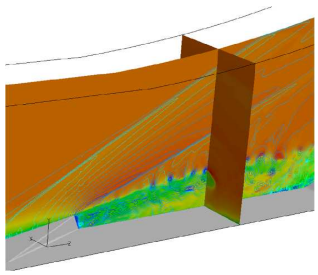

Fig. 4 The instantaneous pressure and streamwise velocity contour on different cross sections.

central plane. From the figure, we can see many vortex rings appear in the circular shapes. After being told the prediction of the vortex rings, the same experimentalists in UT Arlington tried some techniques to validate the discovery. They used techniques of the particle image velocimetry (PIV) and the acetone vapor screen visualization to track the movement of the flow, and specifically the flash of a laser sheet is used to provide the light exposure at the time level of micro seconds. In Figure 6, a typical image at the center plane is presented taken by using PIV and the acetone vapor (Lu et al [10]). It is clearly demonstrated that a chain of vortex rings exist in the flow field after the MVG! And these structures qualitatively resemble that in Figures 5-6.

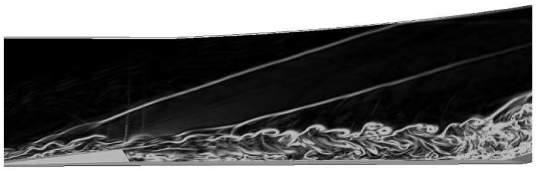

Fig. 5 The numerical shilieren at the center plane.

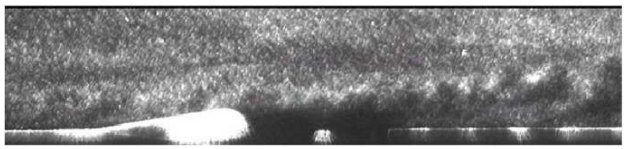

Fig. 6 The laser-sheet flash image at the center plane. Upper: using PIV, lower: using the acetone vapor.

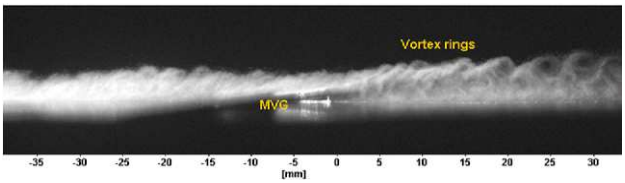

4 Conclusion

Base on numerical results, the inflection points (surface in 3-D) inside the deficit area are found. The mechanism for the vortex rings was analyzed and found that, the existence of the high shear layer and inflection surface generated by the momentum deficit will cause the corresponding Kelvin-Helmholtz instability, which develops into a series of vortex rings. Kelvin-Helmholtz type instability is caused by the momentum deficit. Vortex rings are generated by K-H type instability after MVG. The experiment work demonstrated that a chain of vortex rings exist in the flow field after the MVG, and these structures qualitatively resemble that in numerical simulation.

References

1. Babinsky H., Li Y., and Ford C. W. P. (2009) Microramp Control of Supersonic Oblique Shock-Wave/Boundary-Layer Interactions. AIAA J Vol. 47, No. 3:668-675.
2. Li Q., and Liu C. (2010) LES for Supersonic Ramp Control Flow Using MVG at $M = 2.5$ and $Re_\theta = 1440$. AIAA Paper 592.
3. Ghosh S., Choi J., and Edwards J. R. (2010) Numerical Simulations of the Effects of Micro Vortex Generators Using Immersed Boundary Methods. AIAA J Vol. 48, No. 1.
4. Lee S., and Loth E. (2009) Supersonic Boundary Layer Interactions with Various Micro-Vortex Generator Geometries. AIAA Paper 3712.
5. Lee S., and Loth E. (2010) Microramps Upstream of an Oblique-Shock/Boundary-Layer Interaction. AIAA J Vol. 48, No. 1.
6. Li Q., and Liu C. (2010) Numerical Investigations on the Effects of the Declining Angle of the Trailing-Edge of MVG. AIAA Paper 714.
7. Wu M., and Martin M. P. (1996) Direct Numerical Simulation of Supersonic Turbulent Boundary Layer over a Compression Ramp. AIAA J Vol. 45, No. 4:879-889.
8. Grinstein F. F., Margolin L. G., and Rider W. J. *Implicit Large Eddy Simulation*. Cambridge university press, 2007.
9. Liu C., and Chen L. (2010) Study of Mechanism of Ring-Like Vortex Formation in Late Flow Transition. AIAA Paper 1456.
10. Lu F., Pierce A., and Shih Y.(2010) Experimental Study of Near Wake of Micro Vortex Generators in Supersonic Flow. AIAA Paper 4623.